High-Q Silicon Resonators For High-Coherence Hybrid Si/III-V Semiconductor Lasers

Christos T. Santis, and Amnon Yariv
California Institute of Technology, M/C 128-95, Pasadena, California 91125
christos@caltech.edu

Abstract: We report on the design and experimental demonstration of high-Q Si resonators with Q ~ 10^6, a fundamental figure of merit of the phase coherence of hybrid Si/III-V semiconductor lasers.
OCIS codes: (140.4780) Optical resonators; (140.3410) Laser resonators; (140.5960) Semiconductor lasers

1. Introduction

High-Q optical resonators are utilized in a multitude of shapes and configurations to control and modify the emission of light [1]. One of the most technologically ubiquitous light-emitting resonant systems is that of a III-V-based semiconductor laser, found in the backbone of every optical network. The internal loss, or equivalently the intrinsic Q of a semiconductor laser resonator is, for all intents and purposes, considered a material-determined, immutable parameter, largely legacy of a long established diode design paradigm. This leaves little room, other than the resonator loading, in the way of drastic Q enhancement. Recent advances on the heterogeneous integration of otherwise dissimilar materials [2] have enabled the re-thinking of this popular belief.

The cold cavity Q is directly proportional to the number of coherent quanta (i.e. photons) present intra-cavity in the laser field, at any given injection level. This photon population acts like an optical flywheel, which by virtue of its inertia stabilizes the field against random phase perturbations due to spontaneous emission [3]. Therefore, increasing the laser resonator Q provides a powerful knob for the purification of the emitted light's phase coherence (i.e. linewidth), key parameter for meeting the ever-increasing network bandwidth demand. We recently demonstrated a high-coherence hybrid Si/III-V with a quantum noise-limited linewidth of 18 kHz, based on a high-Q Si resonator with Q ~ 10^6 as an integral cavity element [4]. Here, we describe the design methodology and special considerations involved in the development of this technology.

2. Design

A hybrid platform is produced by the bonding of a SOI wafer to a generic III-V wafer (fig. 1(a)). For a minimum Si layer thickness of ~ 450 nm, a fundamental guided mode can be designed with the bulk of its energy stored in Si (~80%), and sufficiently phase-mismatched from the continuum of III-V slab modes. Under these conditions, the total Q of a hybrid resonator can be approximated as

$$\frac{1}{Q} = \frac{1-\Gamma_{Si}}{Q_{III\text{-}V}} + \frac{\Gamma_{Si}}{Q_{Si}}, \quad (1)$$

where Γ_{Si} is the mode confinement factor in Si, and $Q_{III\text{-}V}^{-1}$, Q_{Si}^{-1} are loss rates associated with III-V and Si respectively. With $Q_{Si} \gg Q_{III\text{-}V}$ and in the limit of $1\text{-}\Gamma_{Si} \ll 1$, Q_{Si} becomes the upper limit of the hybrid resonator Q and hence fundamental figure of merit of the laser's coherence. This limit accounts for all sources of loss present in a Si-based, optical resonant structure (e.g. scattering, radiation and absorption) and as such, a well-established toolset of resonator design and fabrication techniques can be employed to address each one optimally.

A distributed feedback structure is defined by patterning a 1D grating on a Si waveguide. Relatively shallow (25-50 nm) waveguide and grating depths are chosen as conducive to reduced scattering and coupling to radiation. A defect mode is localized via the formation of an extended, quasi-continuous photonic heterostructure [5], here implemented by the tuning of the transverse hole diameter W_y (fig. 1(b)). We choose to work directly in the frequency domain, modulating the photonic frequency band-edge (fig. 1(d)) as a parabolic function of the position along the resonator, to create a harmonic photonic "potential" well:

$$f_v(x) = f_{vo} - \frac{x^2}{L_d^2/4V} + V, \quad (2)$$

where L_d, V are the width and "potential" of the well respectively, f_{vo} is a reference frequency, and "v" for valence denotes the analogy between the lower frequency photonic band-edge and the valence band of a semiconductor crystal. Proper choice of L_d and V ensures that a single defect-mode, in this case of the "acceptor" type, is accommodated in the resonator. Conversion to a hole diameter distribution is accomplished by means of a look-up

978-1-55752-968-8/15/$31.00 ©2015 Optical Society of America

table $f_v(W_y)$, which is built *a priori* by 3D eigen-frequency simulation of a full unit cell (fig. 1(c)), for a large number of W_y. Once a particular photonic well has been defined in the frequency domain, it is mapped to a structural modulation via:

$$f_v(x) \xrightarrow{f_v^{-1}(W_y)} W_y(x). \tag{3}$$

With knowledge of $f_v(x)$ (and $f_c(x)$ by default), the respective functions of the grating coupling coefficient $\kappa(x)$, and wavenumber detuning $\delta(x)$, at any applicable frequency, are readily available. The full resonator can then be solved for its frequency spectrum (fig. 1(d)) and resonant mode field distribution by means of 1D coupled-mode equations. The hybrid combination of 3D unit cell-scale and 1D coupled-mode equation simulation constitutes a reasonable trade-off between speed and accuracy for the particular scale of resonators at hand, while still providing ample physical insight and design freedom. We confirm that, similar to electron wavefunctions in a harmonic potential well, the defect mode of a parabolic photonic well also follows a Gaussian-like spatial distribution, a function well behaved in the Fourier reciprocal space. Using the momentum space as a monitor, L_d and V can be chosen such that high-frequency Fourier components be sufficiently suppressed, thus minimizing coupling to leaky states (fig. 1(e)). The acceptor mode design creates an effective anti-resonance condition for states in the conduction band, resulting in enhanced suppression of otherwise competing side-modes (SMMR > 50 dB).

3. Conclusion

Silicon resonators are tested to assess the overall design scheme and quality of the fabrication process. High-Q Si resonators with Qs exceeding 10^6 are obtained (fig. 1(f)). All in all, this approach proves extremely versatile at the designing of extended, yet single-mode high-Q resonators.

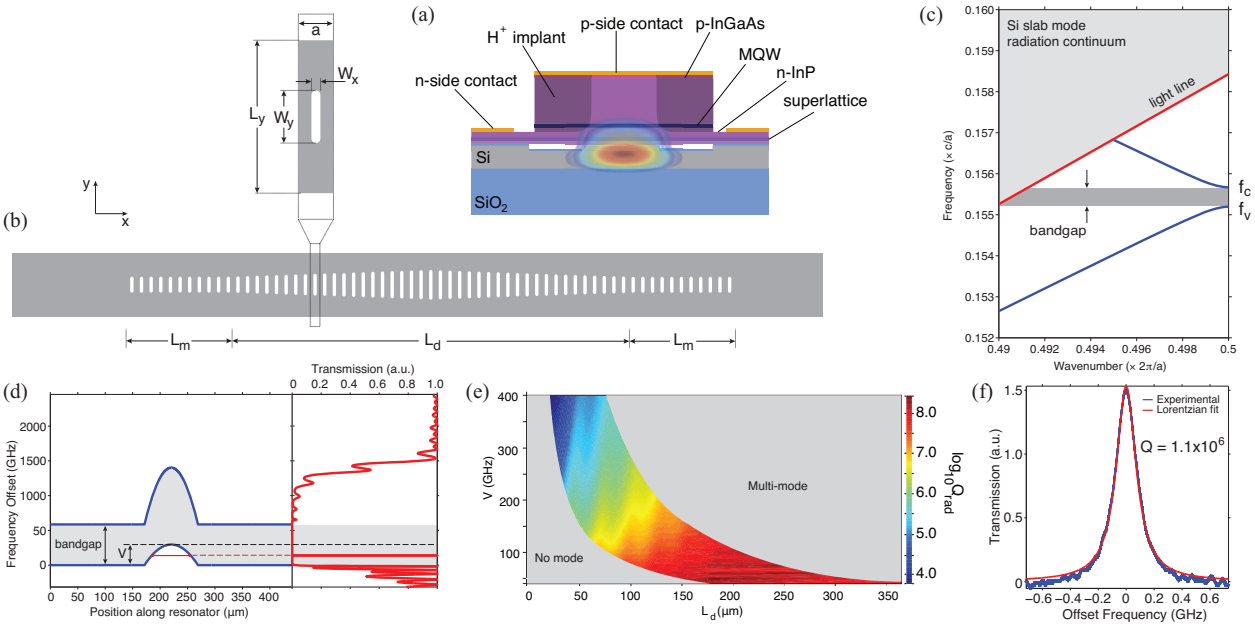

Fig. 1. (a) Hybrid Si/III-V laser cross-section, (b) high-Q Si resonator top view (not to scale), (c) simulated 3D unit cell bandstructure, (d) designed photonic band-edge and calculated transmission frequency spectrum, (e) calculated radiation-limited Q as a function of L_d, V, (f) experimental high-Q Si resonance with Lorentzian fit.

4. References

[1] K. J. Vahala, "Optical microcavities," *Nature,* vol. 424, pp. 839-846, Aug 14 2003.

[2] A. W. Fang, H. Park, O. Cohen, R. Jones, M. J. Paniccia, and J. E. Bowers, "Electrically pumped hybrid AlGaInAs-Silicon evanescent laser," *Optics Express,* vol. 14, pp. 9203-9210, 2006.

[3] C. H. Henry, "Theory of the linewidth of semiconductor lasers," *IEEE J. Quantum Electronics,* vol. 18, pp. 259-264, 1982.

[4] C. T. Santis, S. T. Steger, Y. Vilenchik, A. Vasilyev, and A. Yariv, "High-coherence semiconductor lasers based on integral high-Q resonators in hybrid Si/III-V platforms," *Proceedings of the National Academy of Sciences of the United States of America,* vol. 111, pp. 2879-2884, Feb 25 2014.

[5] B. S. Song, S. Noda, T. Asano, and Y. Akahane, "Ultra-high-Q photonic double-heterostructure nanocavity," *Nature Materials,* vol. 4, pp. 207-210, 2005.